

Stratospheric influence on circulation changes in the Southern Hemisphere troposphere in coupled climate models

A. Yu. Karpechko,¹ N. P. Gillett,¹ G. J. Marshall,² and A. A. Scaife³

Received 15 July 2008; revised 22 August 2008; accepted 9 September 2008; published 18 October 2008.

[1] The recent intensification of the circumpolar circulation in the SH troposphere in summer and autumn has been attributed to external forcing such as stratospheric ozone depletion and greenhouse gas (GHG) increases. Several studies have shown that climate models are able to simulate observed changes when forced by observed ozone trends or combined ozone and GHG trends. However, as some of these studies suffered from erroneously specified forcing, the reason for the circulation intensification remains debatable. Here, we re-approach this issue using data from 21 CMIP3 models. We demonstrate that only models that include ozone depletion simulate downward propagation of the circulation changes from the stratosphere to the troposphere similar to that observed, with GHG increases causing significant Antarctic geopotential height trends only in the lower troposphere. These changes are simulated by the majority of the ozone-forced models except those with the lowest vertical resolution between 300 hPa and 10 hPa. **Citation:** Karpechko, A. Yu., N. P. Gillett, G. J. Marshall, and A. A. Scaife (2008), Stratospheric influence on circulation changes in the Southern Hemisphere troposphere in coupled climate models, *Geophys. Res. Lett.*, 35, L20806, doi:10.1029/2008GL035354.

1. Introduction

[2] The last decades of the 20th century were marked by a significant change in the Antarctic tropospheric circumpolar circulation, with strengthening westerly winds and decreases in Antarctic geopotential height [Thompson and Solomon, 2002, hereinafter referred to as TS02]. The trends have been largest in summer and autumn [cf. Marshall, 2007, Table 1], lagging by 1–2 months similar trends in the stratosphere, which suggests a possible stratosphere-to-troposphere influence. In terms of large-scale modes of atmospheric variability, these changes can be interpreted as a shift towards the positive phase of the Southern Annular Mode (SAM).

[3] An increase of the SAM index has been simulated in General Circulation Model experiments in response to anthropogenic greenhouse gas (GHG) increases [e.g., Fyfe *et al.*, 1999; Kushner *et al.*, 2001] and Antarctic stratospheric ozone depletion [Gillett and Thompson, 2003]. Shindell and Schmidt [2004] and Arblaster and Meehl [2006] used both these factors in coupled models and showed that ozone depletion was the dominant contributor to observed changes

in the mid-troposphere while both GHG and stratospheric ozone forcing played a comparable role at the surface.

[4] So far, the causes of the Antarctic tropospheric trends have been investigated using a single-model approach. The studies of Marshall *et al.* [2004] and Shindell and Schmidt [2004] suffered from erroneously specified ozone forcing. Moreover, Jones and Widmann [2004] suggested that the observed trends are not inconsistent with natural variability. Here we re-approach this issue using simulations of the 20th century performed by all the major coupled models assembled in the CMIP3 database in support of the Intergovernmental Panel of Climate Change Fourth Assessment Report (IPCC AR4). While some of the models account for the stratospheric ozone decline others do not. This gives us an opportunity to isolate the influence of ozone depletion on the troposphere in a multi-model study. Multi-model averages are often more realistic than output from a single model [e.g., Connolley and Bracegirdle, 2007]. Miller *et al.* [2006] and Cai and Cowan [2007] used the CMIP3 data to study sea level pressure (SLP) changes. Here we look at changes throughout the troposphere and the lower stratosphere below 30 hPa. So, the objectives of the present study are: a) assessment of the CMIP3 models' ability to simulate the Antarctic circulation trends, and b) evaluation of the influence of Antarctic stratospheric ozone changes on the tropospheric circulation.

2. Model Data

[5] Data from all CMIP3 models available on pressure levels were retrieved from the World Climate Research Programme's (WCRP's) Coupled Model Intercomparison Project phase 3 (CMIP3) dataset at <https://esgcat.lnl.gov:8443/>. Table 1 gives some information on the models used for this study. Altogether data from 61 simulations by 21 models are used. HadCM3 has ozone forcing twice as large as observed [Gillett and Thompson, 2003] and was therefore excluded from this study. CNRM-CM3 has interactive ozone and was also excluded because our goal is to study the response to the observed forcing. For both GISS-E models data was downloaded directly from the GISS server (<ftp://data.giss.nasa.gov/pub/pcmidi/>) in order to avoid problems associated with erroneously specified ozone forcing in earlier runs included in the CMIP3 database [Miller *et al.*, 2006]. Connolley and Bracegirdle [2007] provide an assessment of CMIP3 model skill at simulating Antarctic climate as well as the surface temperature trends.

3. Results

[6] To isolate the influence of stratospheric ozone depletion, models were divided into two groups according to

¹Climatic Research Unit, University of East Anglia, Norwich, UK.

²British Antarctic Survey, Cambridge, UK.

³Hadley Centre, Met Office, Exeter, UK.

Table 1. Description of CMIP3 Models Used in This Study

Model Name and Country	N runs	Ozone		
		Forcing	Levels	Top
BCCR BCM2.0, Norway	1	No	31	10 hPa
CCCMA CGCM3.1 T47, Canada	5	No	32	1 hPa
CCCMA CGCM3.1 T63, Canada	1	No	32	1 hPa
CSIRO MK3.0, Australia	2	Yes	18	4.5 hPa
CSIRO MK3.5, Australia	1	Yes	18	4.5 hPa
GFDL CM2.0, USA	3	Yes	24	3 hPa
GFDL CM2.1, USA	3	Yes	24	3 hPa
GISS-ER, USA	4	Yes	20	0.1 hPa
GISS-EH, USA	5	Yes	20	0.1 hPa
GISS-AOM, USA	2	No	12	10 hPa
FGOALS-g1.0, China	3	No	26	2.2 hPa
INGV-SXG, Italy	1	Yes	19	10 hPa
INM-CM3.0, Russia	1	No	21	10 hPa
IPSL-CM4, France	2	No	19	32 km
MIROC3.2 (hires), Japan	1	Yes	56	1 hPa
MIROC3.2 (medres), Japan	3	Yes	20	10 hPa
ECHAM5/MPI-OM, Germany	4	Yes	31	10 hPa
MRI CGCM2.3.2, Japan	5	No	30	0.4 hPa
CCSM3.0, USA	8	Yes	26	2.2 hPa
PCM, USA	4	Yes	18	2.9 hPa
UKMO-HadGEM1, UK	2	Yes	38	3.1 hPa

whether or not they include the ozone trends. Figure 1 shows ensemble averaged temperature and geopotential trends in both groups for the period of 1969–1998. Model trends are calculated over the locations of observation stations used by TS02 whose results are shown alongside. To facilitate the comparison with observations, the same period and the same diagnostics were used for the models. Altogether 41 model runs are used to produce the ozone composite and 20 runs for the no-ozone composite. Some of the models do not provide data at the lowest tropospheric levels where they intersect with topography: Data at the 850 hPa level are available from only about a half of the runs indicated above. Surface temperature, available for all simulations, was used in place of 1000 hPa temperature. Geopotential height at the 1000 hPa level was replaced by SLP rescaled using the formula $8*(SLP-1000)$ [Thompson and Wallace, 2000].

[7] Figure 1c, which shows averaged temperature trends for the ozone ensemble, features the well-known springtime lower stratospheric cooling that has previously been attributed to ozone depletion [e.g., Randel and Wu, 1999]. The altitude (100 hPa), the timing (November), and the magnitude (-7.6 K per 30-year) of maximum cooling are in a good agreement with the observations (Figure 1a). In accordance with expectations, the cooling is missing in the no-ozone ensemble average (Figure 1e). Both ensembles reproduce moderate stratospheric cooling throughout the year, which is partly attributable to the GHG increase [e.g., Ramaswamy *et al.*, 2001]. In the no-ozone ensemble the stratospheric cooling has no particular seasonality, with values typically less than 1 K per 30-year. Also, the cooling becomes statistically insignificant during the dynamically active period. This is likely due in part to the higher interannual variability in these months [Shiotani *et al.*, 1993]; although a GHG-induced strengthening of the Brewer-Dobson circulation and associated adiabatic warming in the extratropics could also play a role [Butchart and Scaife, 2001].

[8] Both ensembles simulate tropospheric warming that is attributable to the GHG concentration increase. In the observations, the warming peaks in winter, with values exceeding $+1.5$ K per 30-year, but the models show a more seasonally uniform warming, suggesting that the observed seasonality may be due to internal variability, although possible model imperfections (e.g., unresolved processes) could also be responsible for this discrepancy.

[9] In the ozone ensemble, significant negative geopotential trends are seen above 70 hPa throughout the year and down to the surface in summer (Figure 1d). However, the magnitude of the geopotential height trends is smaller than that observed. At 30 hPa, the trends peak in November while at 100 hPa and below they reach a maximum 1–2 months later. In the following this lagged trend pattern will be referred to as downward trend propagation. At the surface, significant downward trends are reproduced from November to May, in good agreement with the observations (Figure 1b). However we do not see a secondary maximum in geopotential height trends in autumn, as is seen in the observations (Figure 1b), and as was simulated by Keeley *et al.* [2007] using HadSM3-L64.

[10] With regard to the no-ozone ensemble (Figure 1f), one can see that significant geopotential trends in the stratosphere are missing. Nevertheless, weak insignificant negative trends are observed in the upper part of the domain, due to greenhouse cooling which is largest in the upper stratosphere [Ramaswamy *et al.*, 2001]. Negative trends are also observed in the lower troposphere (below 500 hPa) and they are significant at the surface from December to March, consistent with previous studies [Miller *et al.*, 2006; Cai and Cowan, 2007]. The surface trends maximize in summer with a magnitude of about -15 m per 30-year, which is slightly more than a half of the trend in the ozone ensemble (-26 m per 30-year). Since the ozone ensemble models are forced by both GHG increase and ozone depletion this suggests that the contributions of these factors in the lower troposphere are comparable, consistent with Shindell and Schmidt [2004].

[11] Having shown that the observed trend pattern is reproduced by the ozone ensemble average, we turn to the question of how the individual models simulate the observed changes. The above analysis was repeated for each model separately. We identified which models simulate downward propagation by testing whether the seasonal mean geopotential height trends at 500 hPa in December–January exceed one standard deviation of the season-to-season variability, following TS02. Although the no-ozone ensemble average revealed no significant trends above 800 hPa, each model member of this group was also checked separately. No model without ozone trends reproduces significant December–January geopotential height trends at 500 hPa although four models (CCCMA CGCM3.1 T63, FGOALS-g1.0, INM-CM3.0, and MRI CGCM2.3.2) show negative trends. Averaging over these models produces negative trends throughout the troposphere in summer and they are significant below 400 hPa but not significant in the upper troposphere. Among ozone forcing models only CSIRO models (both 3.0 and 3.5 versions) and GFDL models (both 2.0 and 2.1 versions) fail to simulate the downward trend propagation. These models have relatively poor vertical resolution in the lower stratosphere. Figure 2

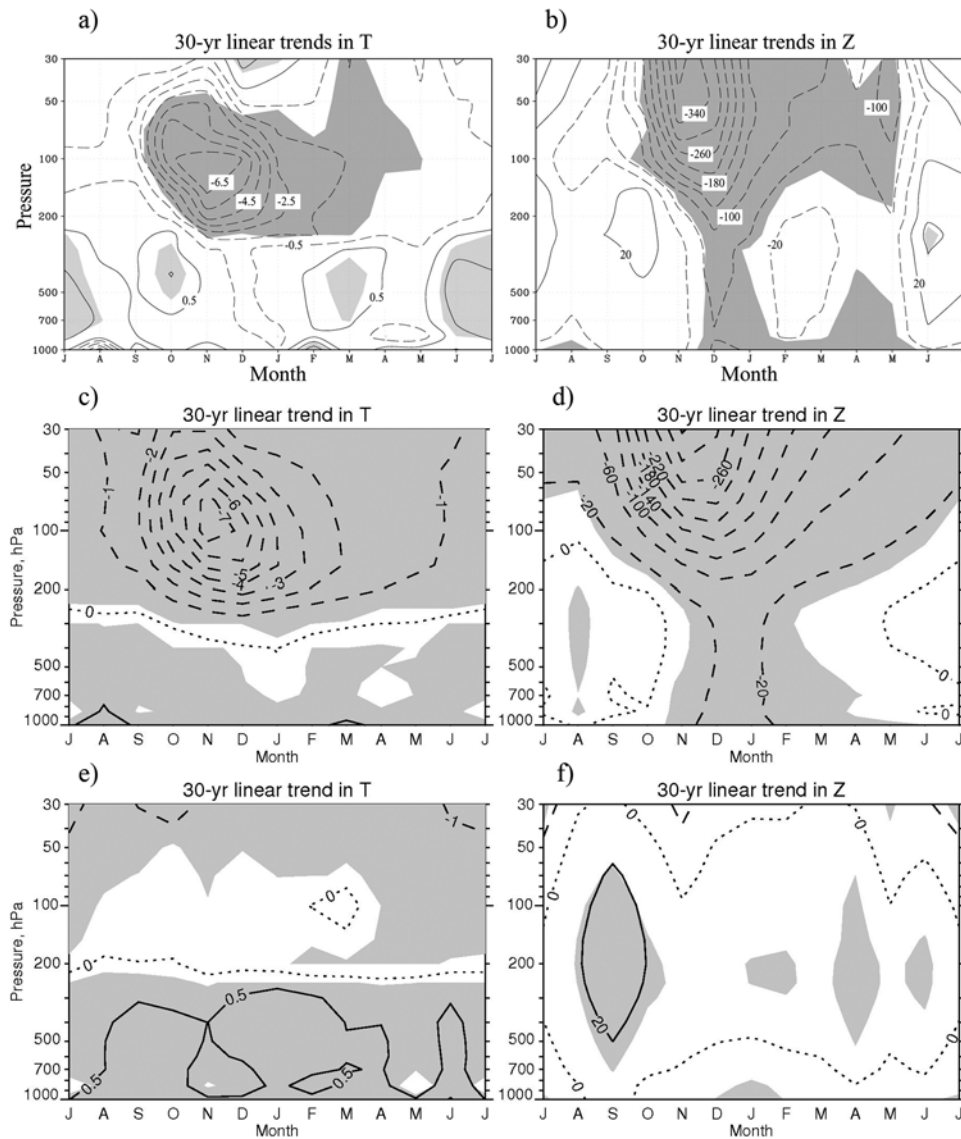


Figure 1. Seasonal cycle of linear trends in (left) temperature (K per 30 years) and (right) geopotential height (m per 30 years) over the Antarctic: (a)–(b) observations, (c)–(d) ozone ensemble average, and (e)–(f) no-ozone ensemble average. Shading denotes trends that exceeded 1SD of the respective monthly time series.

shows the vertical level structure of the ozone ensemble models. Models are sorted from left to right in accordance to their number of levels between 300 hPa and 10 hPa. It is seen that the CSIRO and GFDL models have the lowest resolution in this region.

[12] The models are separated into a low vertical resolution ensemble (LOW) consisting of both CSIRO and GFDL models and a high vertical resolution ensemble (HIGH) that consists of the rest of the models from the ozone ensemble. Thus, the LOW models have 6 or fewer levels in the height interval between 300 hPa and 10 hPa and the HIGH models have 7 or more levels. The LOW ensemble consists of 9 simulations while the HIGH ensemble consists of 32 simulations. Subdivision of the HIGH ensemble into groups of models with at least 12 levels and models with fewer than 12 levels between 300 hPa and 10 hPa revealed no significant differences in geopotential height trends between these two groups.

[13] Figure 3 shows that in the stratosphere HIGH and LOW models perform rather similarly. In both ensembles, maximum cooling is simulated in November at 100 hPa and is of similar magnitude in each (-7.7 K in the HIGH ensemble and -7.3 K in the LOW ensemble). Note that cooling in the GFDL CM2.0 model is only -3.4 K per 30-year meaning that this model does not capture the magnitude of cooling correctly. Excluding this model from the LOW ensemble produces results similar to those shown. In the HIGH ensemble (Figure 3c), cooling propagates down to 700 hPa in summer as in observations. The LOW ensemble (Figure 3a) simulates tropospheric warming with a maximum in spring exceeding 0.5 K per 30-year.

[14] In both ensembles, negative trends in the stratospheric geopotential height are observed in spring although in the LOW ensemble they are of slightly smaller magnitude. The difference becomes clearer in the troposphere where no sign of the downward trend propagation is evident in the LOW

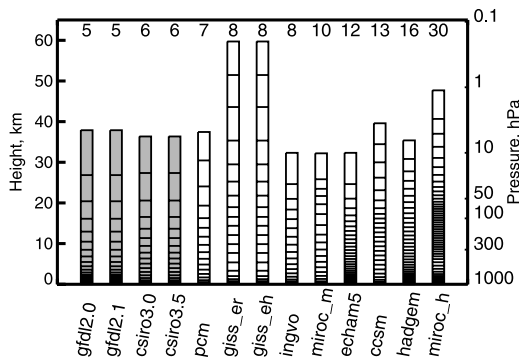


Figure 2. Structure of vertical levels in ozone ensemble models. Approximate heights of the midpoints of the layers are shown. Models which do not simulate the downward trend propagation are shaded. Numbers above the bars indicate the number of levels between 300 hPa and 10 hPa.

ensemble (Figure 3b). However, significant negative geopotential height trends are observed at the surface with a magnitude of -14 m per 30-year which is comparable to that in the no-ozone ensemble. The similarity in tropospheric geopotential responses between the LOW ensemble and the no-ozone ensemble suggests that the stratospheric influence is not communicated to the troposphere in the low resolution models and that the tropospheric response in these models is due to GHG forcing only. Since the LOW models might be expected to simulate radiative processes coupling the stratosphere and troposphere well, but perhaps not the

dynamical processes [Gillett *et al.*, 2003], this provides evidence in favor of dynamical processes being the dominant drivers of the tropospheric response to stratospheric ozone depletion.

[15] Figure 2 also suggests that a high model top is not a necessary factor for the correct capturing of the stratosphere-troposphere coupling, since models with a relatively low upper boundary (ECHAM5/MPI-OM, INGV-SXG, MIROC3.2 (medres)) simulate the downward trend propagation. Note that the models that don't simulate the downward propagation have intermediate upper boundary heights (Table 1).

4. Discussion and Conclusions

[16] Our results demonstrate that both ozone depletion and GHG increases have played a role in the observed decrease of tropospheric geopotential height over the Antarctic. At the surface, their contributions are comparable while in the upper troposphere the ozone contribution dominates. In the future, Miller *et al.* [2006] found that the SAM index will continue to increase as a response to projected GHG concentration, whereas chemistry climate models predict a decrease of the SAM index during austral summer due to the expected ozone recovery despite increasing GHG concentrations [Perlwitz *et al.*, 2008; Son *et al.*, 2008], thus implying dominance of the ozone contribution for future summer SAM trends.

[17] While ozone depletion naturally acts on the tropospheric circulation through stratosphere-troposphere coupling there is no consensus on how the GHG increase acts. Shindell *et al.* [1999] proposed a mechanism that

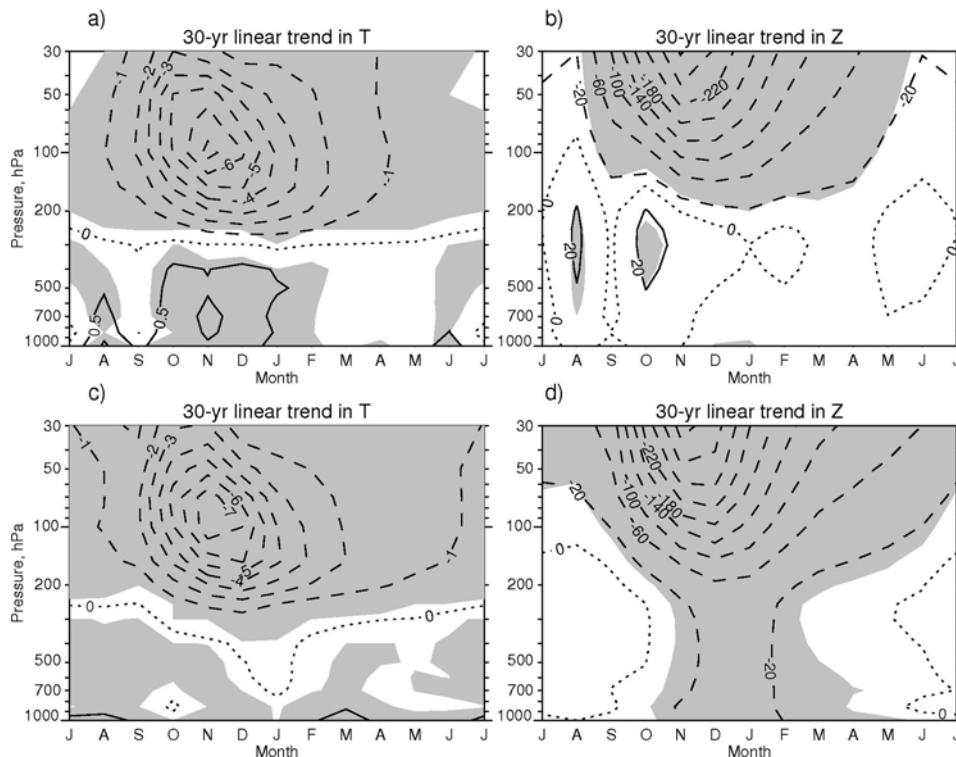


Figure 3. The same as Figure 1 except for (a)–(b) low resolution group average and (c)–(d) high resolution group average. Shading denotes trends that exceed 1SD of the respective monthly time series.

involved enhanced planetary wave refraction in the stratosphere towards the equator. Alternative hypotheses relate the SAM increase to an increased meridional temperature gradient or warming of the ocean surface [see Cai *et al.*, 2003, and references therein]. Our results, which show that the significant Antarctic geopotential height decreases simulated in response to GHG increases do not extend to the upper troposphere, do not support the theory relying on the downward influence of GHG-induced changes in the stratosphere.

[18] There is also no consensus on the mechanisms by which the stratosphere influences the troposphere [Thompson *et al.*, 2006]. Present results demonstrate that the models with low vertical resolution in the lower stratosphere (below 10 hPa) do not reproduce the tropospheric response to ozone depletion in the Antarctic. While other features of individual models, like the orographic gravity wave drag in the stratosphere [Sigmond *et al.*, 2008], may also be important for simulating downward trend propagation, our results suggest that vertical resolution in the lower stratosphere plays a dominant role across the CMIP3 ensemble. On the other hand, we show that a high model top is not needed for the simulation of downward trend propagation. This is in agreement with Gillett *et al.* [2003] who showed that the SLP response to stratospheric ozone depletion is sensitive to model resolution below 10 hPa, though not above this.

[19] In summary, using output from 21 CMIP3 models we confirm previous findings based on single models that stratospheric ozone depletion must be accounted for in order to explain the observed temperature and geopotential height trend patterns throughout the Antarctic troposphere during last 30-year period of 20th century. Antarctic geopotential height decreases in response to GHG increases are significant in the lower troposphere. We also conclude that the processes responsible for communication of the ozone depletion signal to the troposphere are not resolved by those climate models that have low vertical resolution in the lower stratosphere.

[20] **Acknowledgments.** This work is supported by NERC Project NE/E006787/1. AS was supported by the Defra and MoD Integrated Climate Programme - GA01101, CBC/2B/0417_Annex C5. NPG was also supported by the Leverhulme Trust. We acknowledge the modeling groups, the Program for Climate Model Diagnosis and Intercomparison (PCMDI) and the WCRP's Working Group on Coupled Modelling (WGCM) for their roles in making available the WCRP CMIP3 multi-model dataset. Support of this dataset is provided by the Office of Science, U.S. Department of Energy. We thank Phil Rasch, Lawrence Boja, and Gary Strand for providing information on CCSM3 and PCM and Seok-Woo Son for a useful comment.

References

Arblaster, J. M., and G. A. Meehl (2006), Contributions of external forcings to southern annular mode trends, *J. Clim.*, *19*, 2896–2905.

Butchart, N., and A. A. Scaife (2001), Removal of chlorofluorocarbons by increased mass exchange between the stratosphere and troposphere in a changing climate, *Nature*, *410*, 799–802.

Cai, W., and T. Cowan (2007), Trends in Southern Hemisphere circulation in IPCC AR4 models over 1950–99: Ozone depletion versus greenhouse forcing, *J. Clim.*, *20*, 681–693, doi:10.1175/JCLI4028.1.

Cai, W., P. H. Whetton, and D. J. Karoly (2003), The response of the Antarctic Oscillation to increasing and stabilized atmospheric CO₂, *J. Clim.*, *16*, 1525–1538.

Connolley, W. M., and T. J. Bracegirdle (2007), An Antarctic assessment of IPCC AR4 coupled models, *Geophys. Res. Lett.*, *34*, L22505, doi:10.1029/2007GL031648.

Fyfe, J. C., G. Boer, and G. Flato (1999), The Arctic and Antarctic oscillations and their projected changes under global warming, *Geophys. Res. Lett.*, *26*, 1601–1604.

Gillett, N. P., and D. W. J. Thompson (2003), Simulation of recent Southern Hemisphere climate change, *Science*, *302*, 273–275, doi:10.1126/science.1087440.

Gillett, N. P., M. R. Allen, and K. D. Williams (2003), Modelling the atmospheric response to doubled CO₂ and depleted stratospheric ozone using a stratosphere-resolving coupled GCM, *Q. J. R. Meteorol. Soc.*, *129*, 947–966.

Jones, J. M., and M. Widmann (2004), Early peak in Antarctic Oscillation index, *Nature*, *432*, 289–290, doi:10.1038/432290b.

Keeley, S. P. E., N. P. Gillett, D. W. J. Thompson, S. Solomon, and P. M. Forster (2007), Is Antarctic climate most sensitive to ozone depletion in the middle or lower stratosphere?, *Geophys. Res. Lett.*, *34*, L22812, doi:10.1029/2007GL031238.

Kushner, P. J., I. M. Held, and T. L. Delworth (2001), Southern Hemisphere atmospheric circulation response to global warming, *J. Clim.*, *14*, 2238–2249.

Marshall, G. J. (2007), Half-century seasonal relationships between the Southern Annular Mode and Antarctic temperatures, *Int. J. Climatol.*, *27*, 373–383.

Marshall, G. J., P. A. Stott, J. Turner, W. M. Connolley, J. C. King, and T. A. Lachlan-Cope (2004), Causes of exceptional atmospheric circulation changes in the Southern Hemisphere, *Geophys. Res. Lett.*, *31*, L14205, doi:10.1029/2004GL019952.

Miller, R. L., G. A. Schmidt, and D. T. Shindell (2006), Forced annular variations in the 20th century Intergovernmental Panel on Climate Change Fourth Assessment Report models, *J. Geophys. Res.*, *111*, D18101, doi:10.1029/2005JD006323.

Perlwitz, J., S. Pawson, R. L. Fogt, J. E. Nielsen, and W. D. Neff (2008), Impact of stratospheric ozone hole recovery on Antarctic climate, *Geophys. Res. Lett.*, *35*, L08714, doi:10.1029/2008GL033317.

Ramaswamy, V., et al. (2001), Stratospheric temperature trends: Observations and models simulations, *Rev. Geophys.*, *39*, 71–122.

Randel, W. J., and F. Wu (1999), Cooling of the Arctic and Antarctic polar stratospheres due to ozone depletion, *J. Clim.*, *12*, 1467–1469.

Shindell, D. T., and G. A. Schmidt (2004), Southern Hemisphere climate response to ozone changes and greenhouse gas increases, *Geophys. Res. Lett.*, *31*, L18209, doi:10.1029/2004GL020724.

Shindell, D. T., R. L. Miller, G. Schmidt, and L. Pandolfo (1999), Simulation of the Arctic Oscillation trend by greenhouse forcing of a stratospheric model, *Nature*, *399*, 452–455.

Shiotani, M., N. Shimoda, and I. Hirota (1993), Interannual variability of the stratospheric circulation in the Southern Hemisphere, *Q. J. R. Meteorol. Soc.*, *119*, 531–546.

Sigmond, M., J. F. Scinocca, and P. J. Kushner (2008), Impact of the stratosphere on tropospheric climate change, *Geophys. Res. Lett.*, *35*, L12706, doi:10.1029/2008GL033573.

Son, S.-W., L. M. Polvani, D. W. Waugh, H. Akiyoshi, R. Garcia, D. Kinnison, S. Pawson, E. Rozanov, T. G. Shepherd, and K. Shibata (2008), The impact of stratospheric ozone recovery on the Southern Hemisphere Westerly Jet, *Science*, *320*, 1486–1489, doi:10.1126/science.1155939.

Thompson, D. W. J., and S. Solomon (2002), Interpretation of recent Southern Hemisphere climate change, *Science*, *296*, 895–899, doi:10.1126/science.1069270.

Thompson, D. W. J., and J. M. Wallace (2000), Annular modes in the extratropical circulation. part I: Month-to-month variability, *J. Clim.*, *13*, 1000–1016.

Thompson, D. W. J., J. C. Furtado, and T. G. Shepherd (2006), On the tropospheric response to anomalous stratospheric wave drag and radiative heating, *J. Atmos. Sci.*, *63*, 2616–2629.

N. P. Gillett and A. Yu. Karpechko, Climatic Research Unit, University of East Anglia, Norwich NR4 7TJ, UK. (a.karpechko@uea.ac.uk)

G. J. Marshall, British Antarctic Survey, Cambridge CB3 0ET, UK.

A. A. Scaife, Hadley Centre, Met Office, Exeter EX1 3PB, UK.